***New Phytologist* Supporting Information**

Article Title: Argonaute7 (AGO7) optimizes arbuscular mycorrhizal fungal associations and enhances competitive growth in *Nicotiana attenuata*

Authors: Maitree Pradhan, Ian T. Baldwin, Shree P. Pandey

Article acceptance date: 02 July 2023

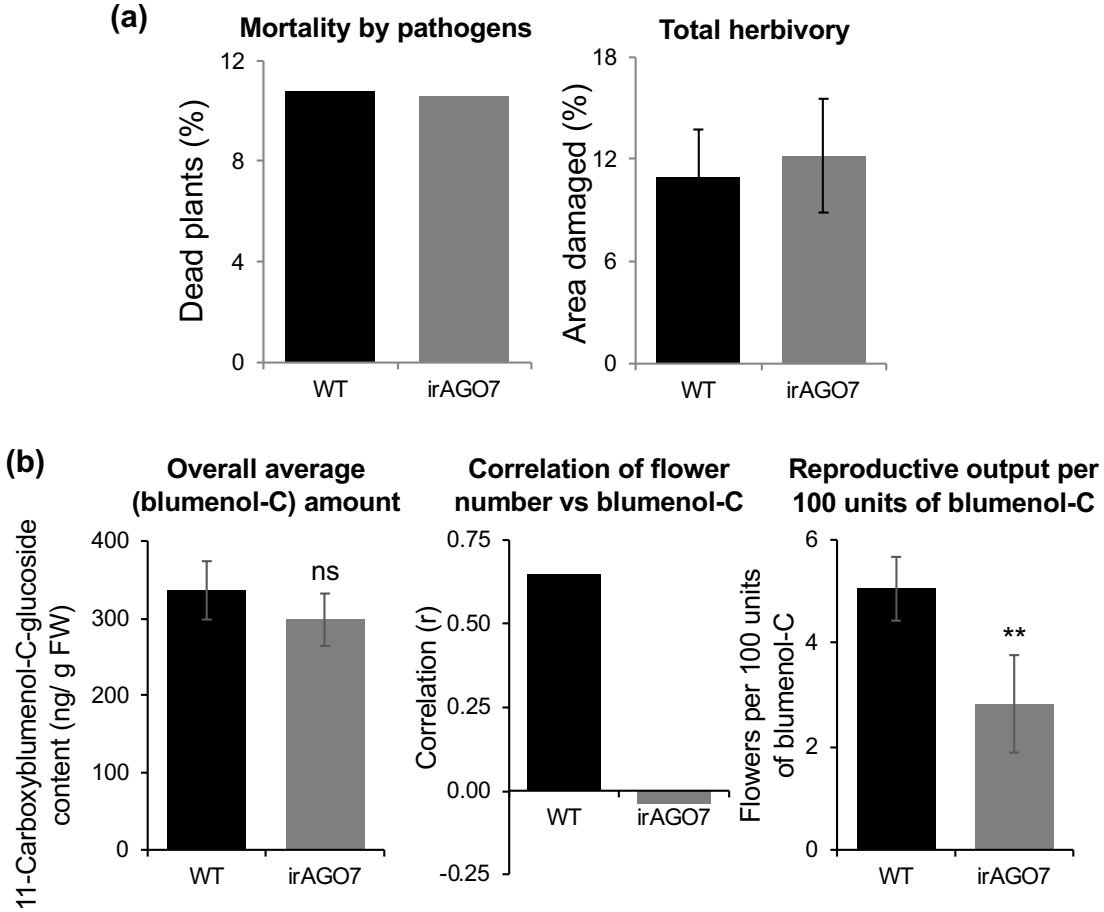

Fig. S1. Evaluation of irAGO7 plants grown in the field. **(a)** WT and irAGO7 plants did not show any significant differences in their susceptibility to natural pathogens (left) or herbivores (right panel). **(b)** Field grown WT and irAGO7 plants were evaluated for AMF. Overall averages of 11-carboxyblumenol-c glucoside (blumenol-C) contents in the leaves of WT and irAGO7 did not differ significantly (left panel; paired t-test, P>0.05; ns). While the WT plants displayed a strong positive correlation (of R^2=0.65) between their reproductive output (flower numbers) and AMF (blumenol-C) content, it was lost in irAGO7 plants, which displayed a negative trend (middle panel). Consequently, the reproductive output per 100 units of blumenol-C was nearly half in irAGO7 as compared to WT plants (** significantly different; paired t-test, n=19 pairs, P=0.016). Error bars represent SEs.

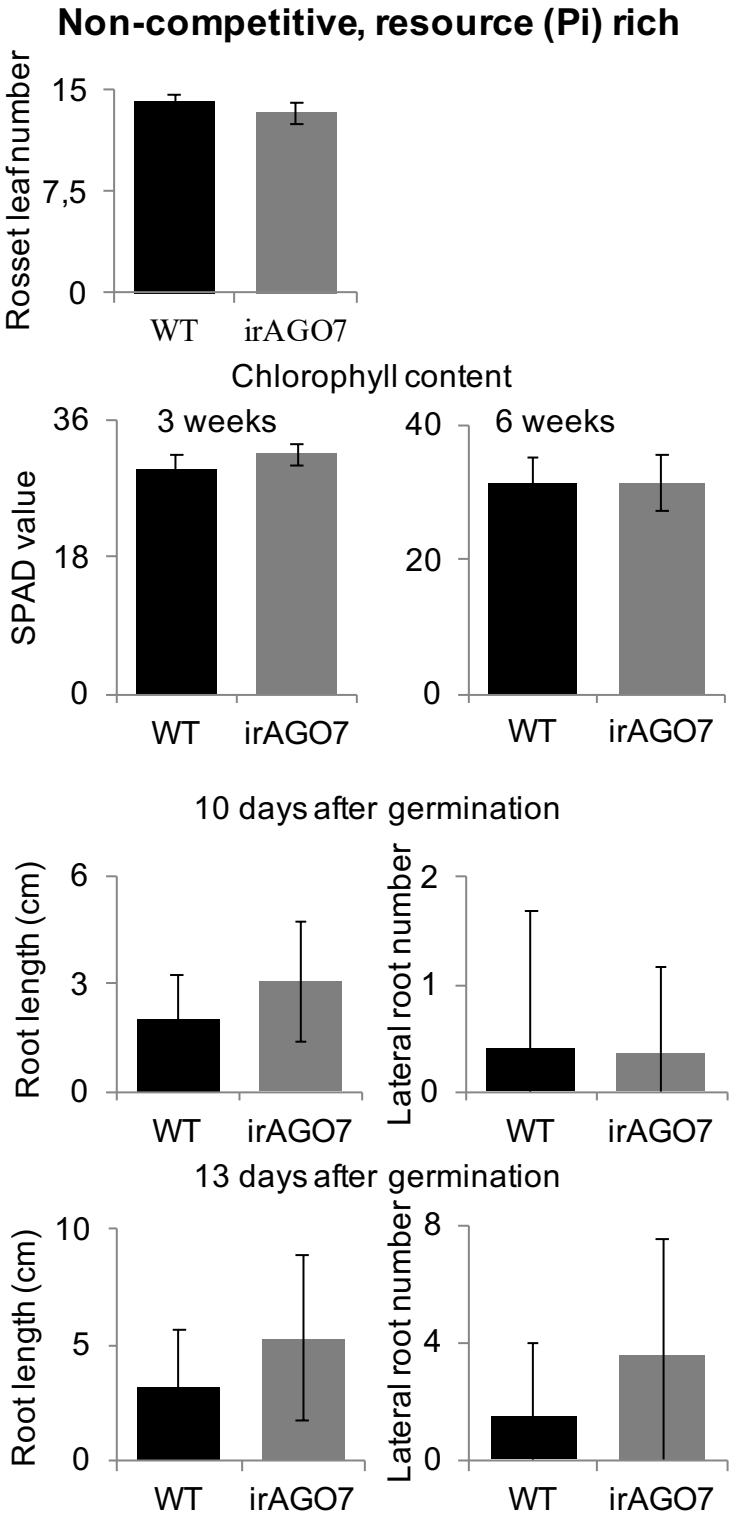

Fig. S2. Glasshouse studies suggest that ir*AGO7* and WT plants have similar rosette leaf numbers, chlorophyll contents, as well as roots (root length or lateral root numbers). Values presented are means ± SD, n=15 biological replicates per genotype for leaf phenotypes and n=30 for root phenotyping (paired t-test, P>0.05).

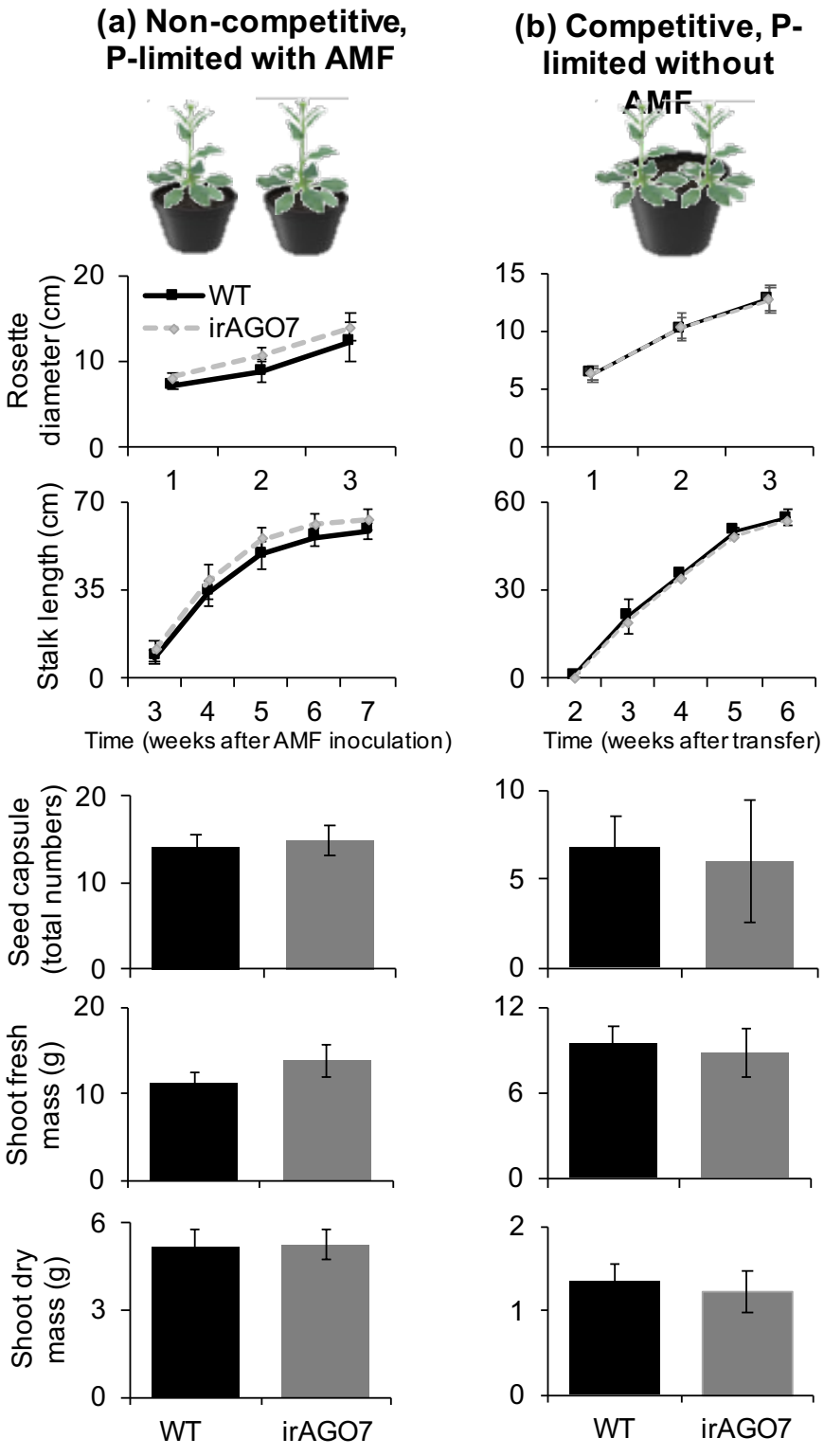

Fig. S3. Silencing *AGO7* does not affect plant growth and fitness when grown under non-competitive, P-limited conditions with AMF (a; n=10), or competitive, P-limited conditions without AMF (b, n=6). Rosette diameter (repeated measures ANOVA, P>0.05), stalk length (repeated measures ANOVA, P>0.05), total seed capsule number (paired t-test, P>0.05), shoot fresh mass (paired t-test, P>0.05) and shoot dry mass (paired t-test, P>0.05) of irAGO7 and WT plants did not differ significantly.

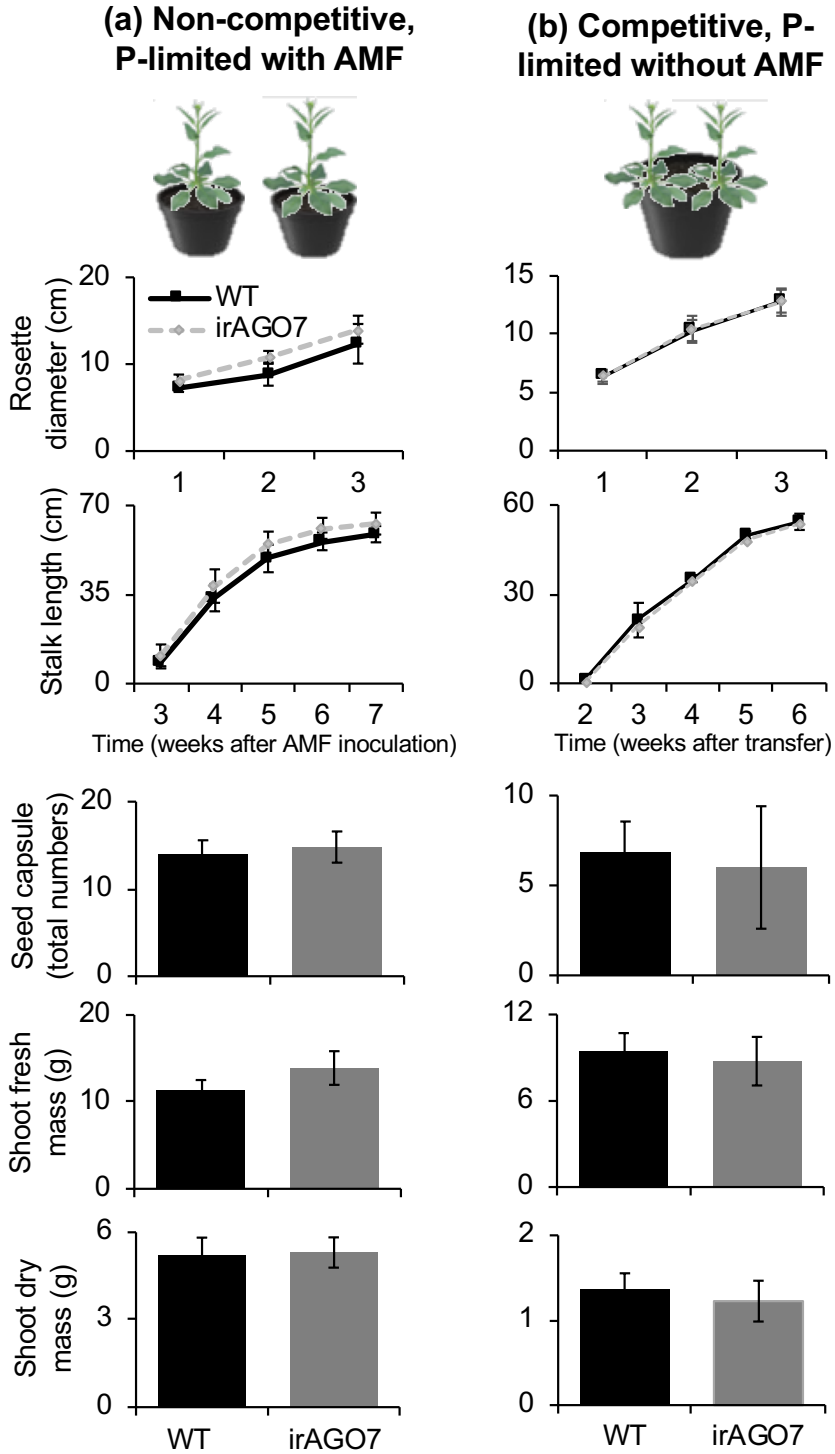

Fig. S4. Silencing *AGO1, 2, 4* or *10* does not affect competitive plant fitness or AMF colonization rates in *N. attenuata* in competitive P-limited conditions identical to those in Fig. **2C,** and Fig. **3**. A minimum decrease of >50% in transcript levels was observed in irAGO lines. A consensus sequence was used to silence the three AGO1 genes (AGO1a, b, c). Further details of generation and characterization of irAGO lines is provided in Pradhan *et al.* (2017). Rosette diameter, stalk length, capsule production and AMF colonization between the WT and isogenic *irAGO* plants were comparable, indicating a lack of significant biological roles for these AGOs in competitive fitness or AMF colonization. Values presented are means ± SD, where n=15 biological replicates per genotype.

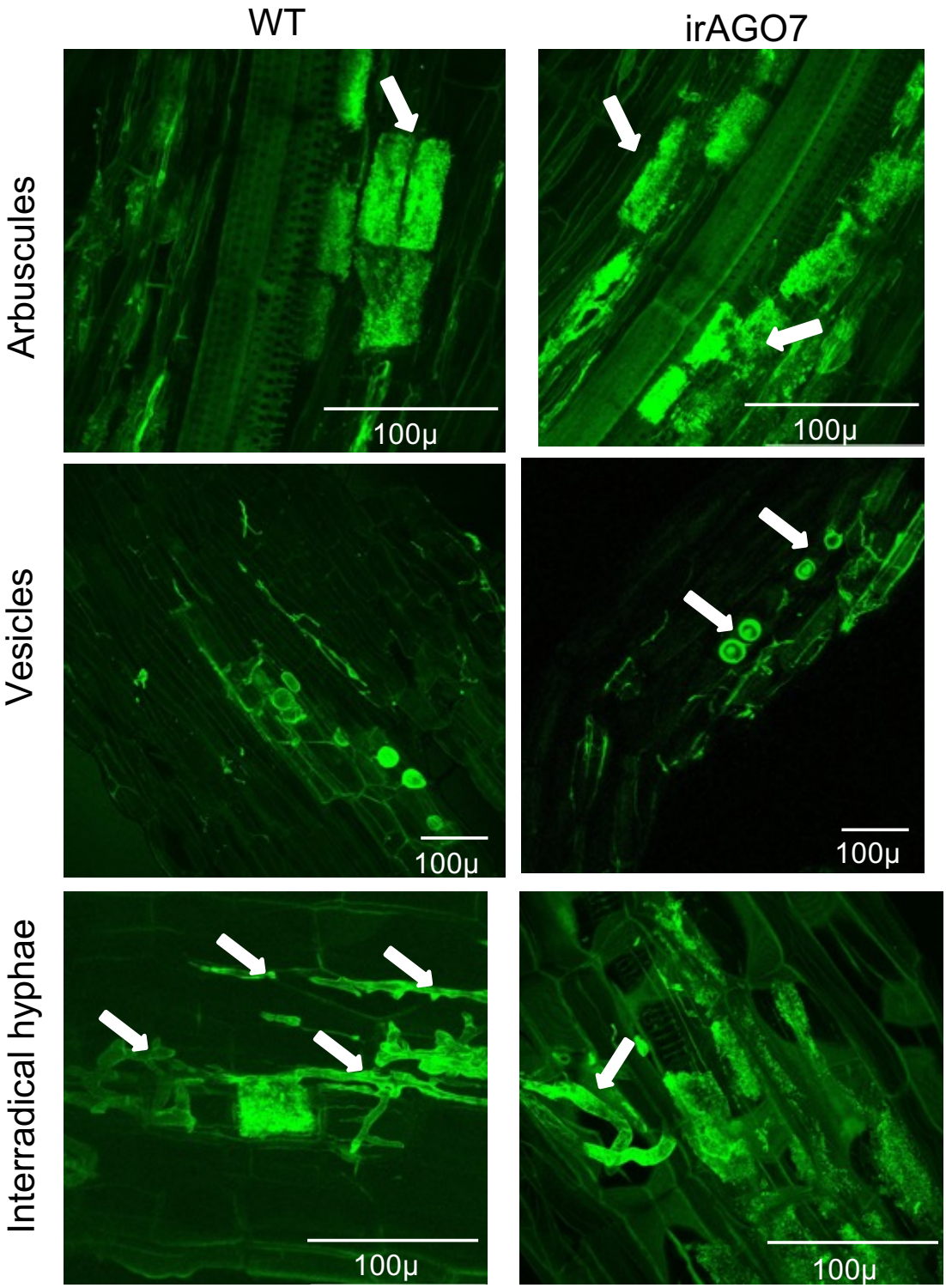

Fig. S5. Microscopic examination of AMF-colonized roots of WT and irAGO7 plants with the help of WGA-fluorescein staining. White arrows indicate arbuscules, vesicles and interradical hypae in the respective pictures. The staining was conducted on samples collected at a time-point of 6-weeks after inoculation.

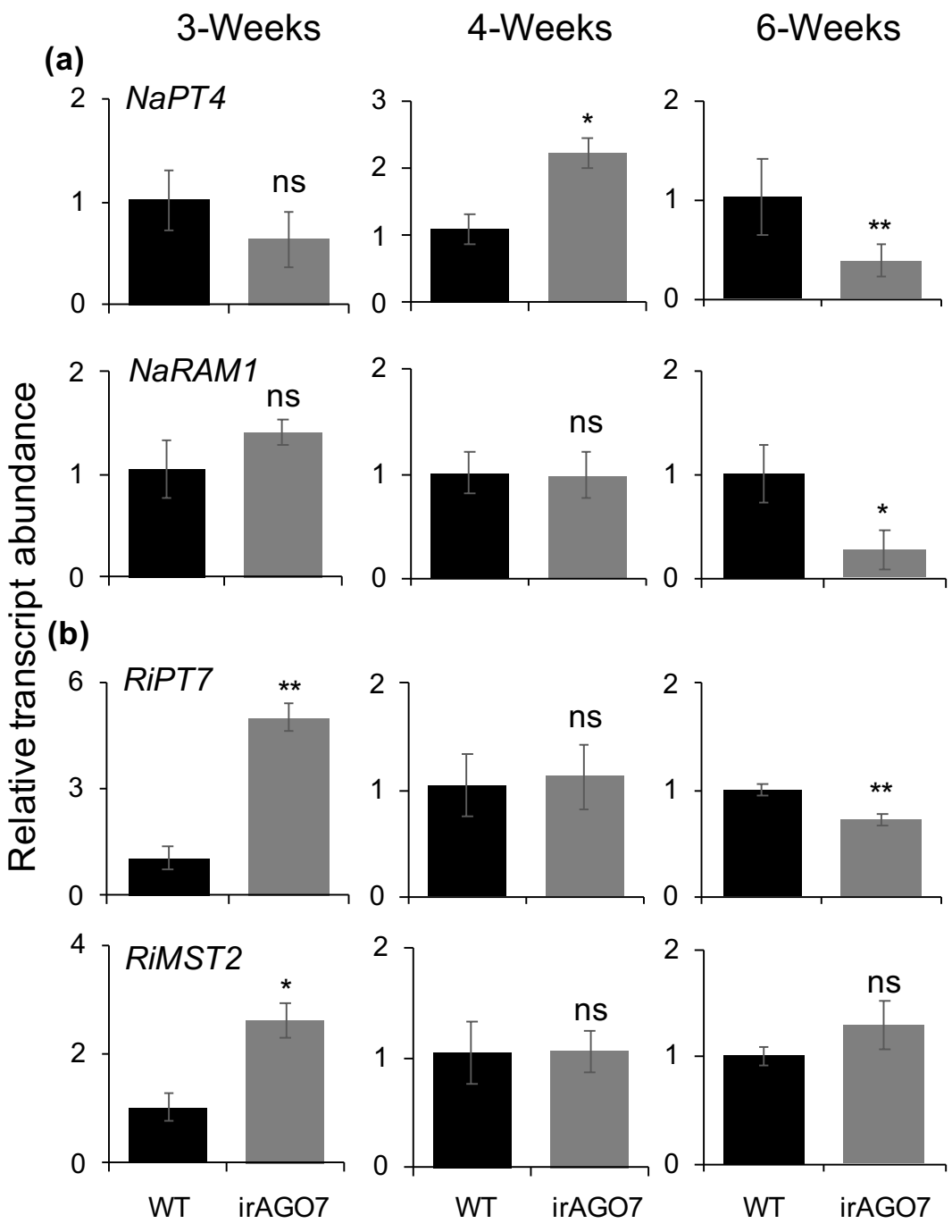

Fig. S6. Transcript abundances of transporter genes relevant for a functional plant-AMF interaction. WT and irAGO7 plants were competitive grown in presence of AMF. Roots samples were collected at 3-, 4- and 6-weeks post inoculation and transcript abundances of **(a)** a phosphate transporter (*PT4*) and the *RAM1* transcription factor of the *N. attenuata* host, and **(b)** a *R. irregularis* phosphate transporter (*RiPT7*) and a monosaccharide transporter (*RiMST2*) were evaluated with the help of quantitative real time PCR assays. For plant genes, *NaECI* gene was used as an internal control, whereas, *RiTEF1* gene was used for fungal transporters. Levels in WT samples were set to 1 and relative accumulation in irAGO7 samples were calculated. Significance was tested with the help of paired t-test. *, ** indicate $P<0.05$ and <0.01, respectively, ns indicated no significant differences.

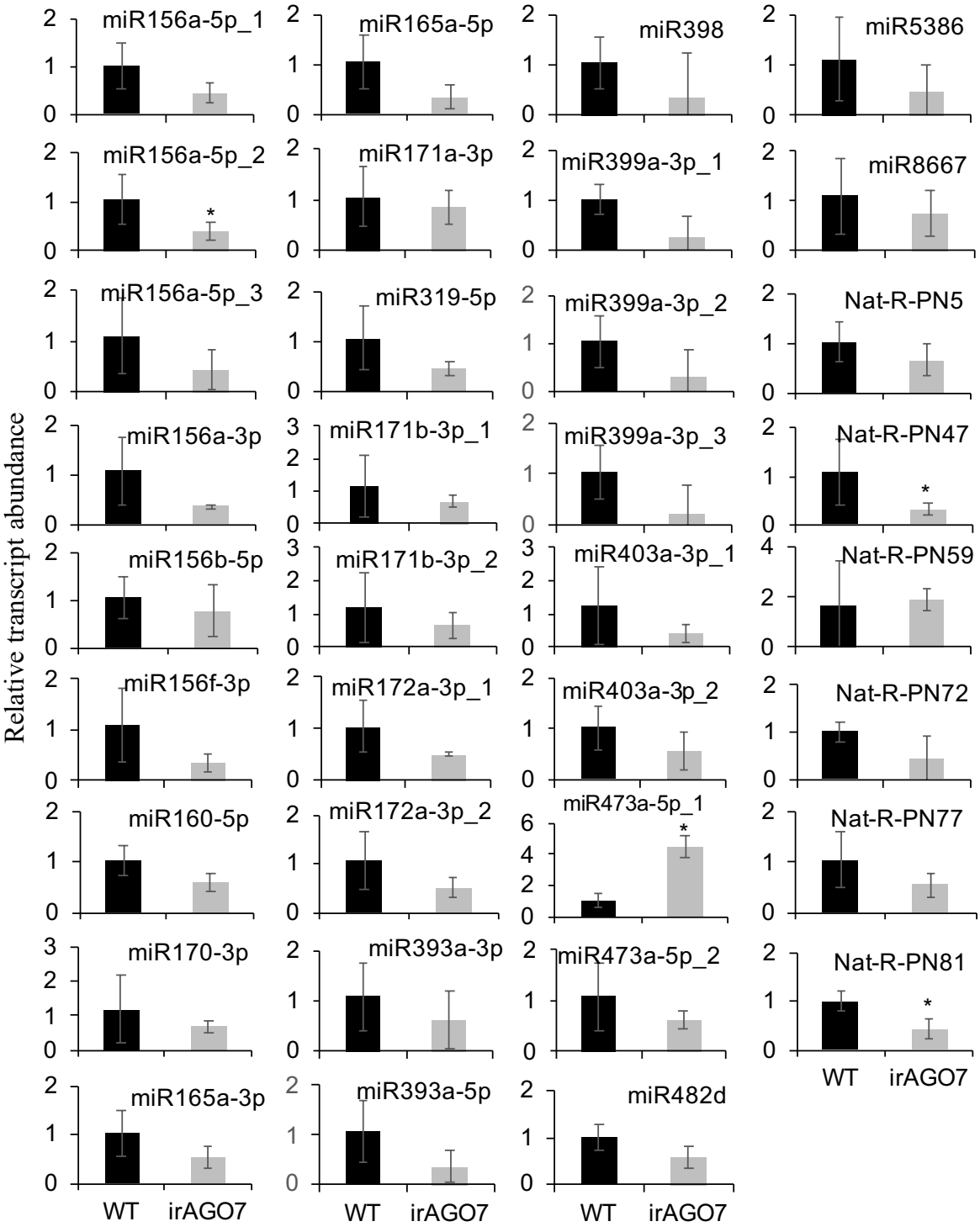

Fig. S7. miRNA accumulation in WT and irAGO7 roots at the time of AMF-inoculation (t_0) using quantitative real time PCR assays. Significance of differences in levels in two genotypes was evaluated with the help of ANOVA at $P<0.05$. Levels in WT were set to 1 and relative accumulation in irAGO7 was calculated. Values indicate mean and error bars indicate SDs.

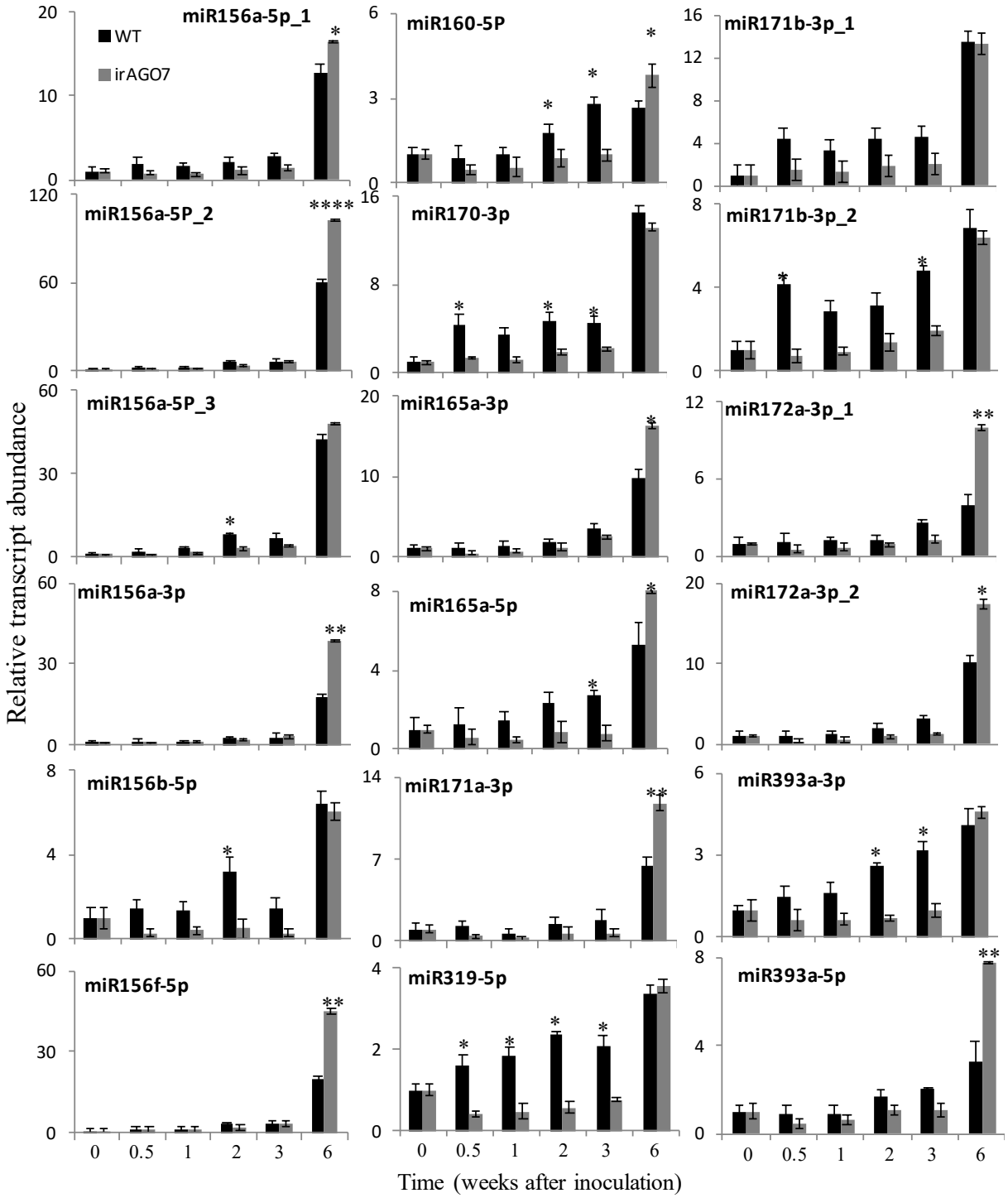
miR156a-5p_1
WT
irAGO7
miR160-5P
miR171b-3p_1
miR156a-5P_2
miR170-3p
miR171b-3p_2
miR156a-5P_3
miR165a-3p
miR172a-3p_1
miR156a-3p
miR165a-5p
miR172a-3p_2
miR156b-5p
miR171a-3p
miR393a-3p
miR156f-5p
miR319-5p
miR393a-5p
Relative transcript abundance
0 0.5 1 2 3 6
Time (weeks after inoculation)

Continued…

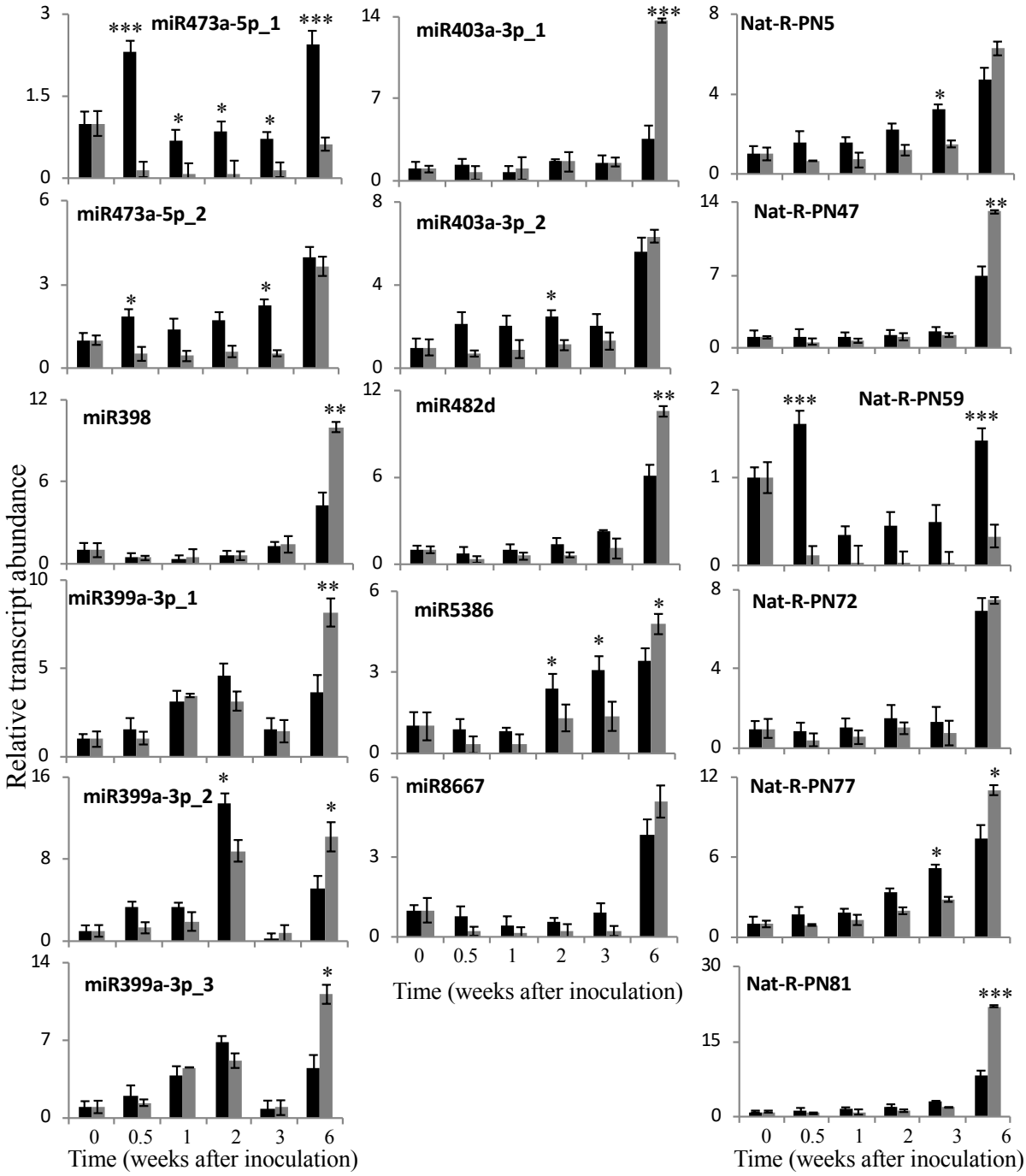

Fig. S8. Temporal dynamics of miRNA accumulation in WT and ir*AGO7* roots during AMF colonization using quantitative real time PCR (qPCR) analysis. Data presented here are related to Fig. 5. Transcript levels at t_0 were set to 1 and relative abundances were calculated accordingly at other time points in both the genotypes. Significant differences were evaluated with the help of two-way repeated measures ANOVA, Fisher's LSD; * $P \leq 0.05$, ** $P \leq 0.01$, *** $P \leq 0.001$ between ir*AGO7* and WT. Values presented are means ± SD, n=3 biological replicates per genotype.

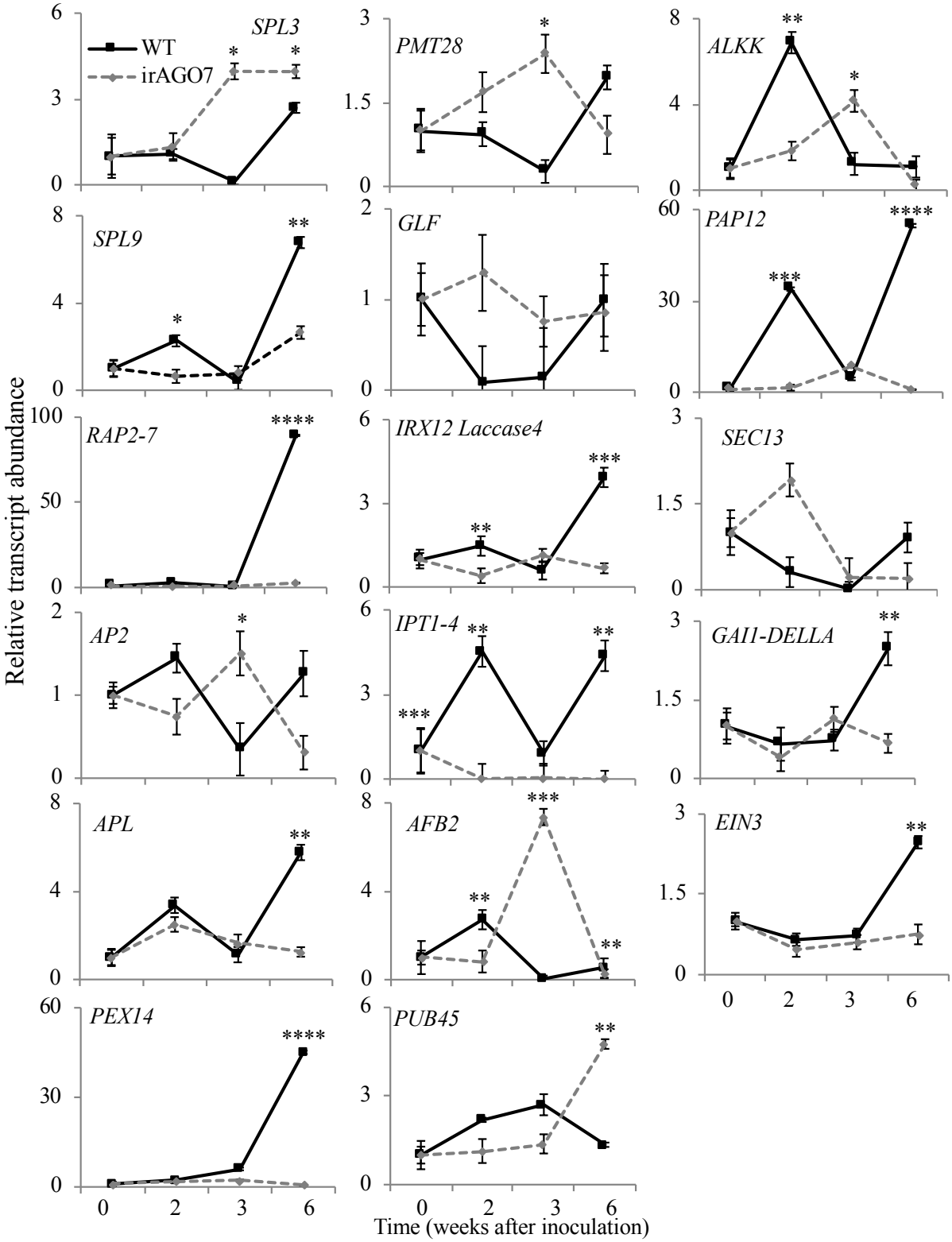

Fig. S9. Elicitation dynamics of putative target genes in AMF inoculated roots of WT and ir*AGO7*. Transcripts of ECI gene were used as internal control for normalization. Data presented here are related to Fig. 5. Transcript level at t_0 was set to 1 and relative abundances were calculated accordingly (significantly different from the respective WT, two-way repeated measures ANOVA (Fisher's LSD; $P \leq 0.05$ *, $P \leq 0.01$ **, $P \leq 0.001$ ***, $P \leq 0.0001$ ****). Values presented are means ± SD, n=3 biological replicates per genotype.

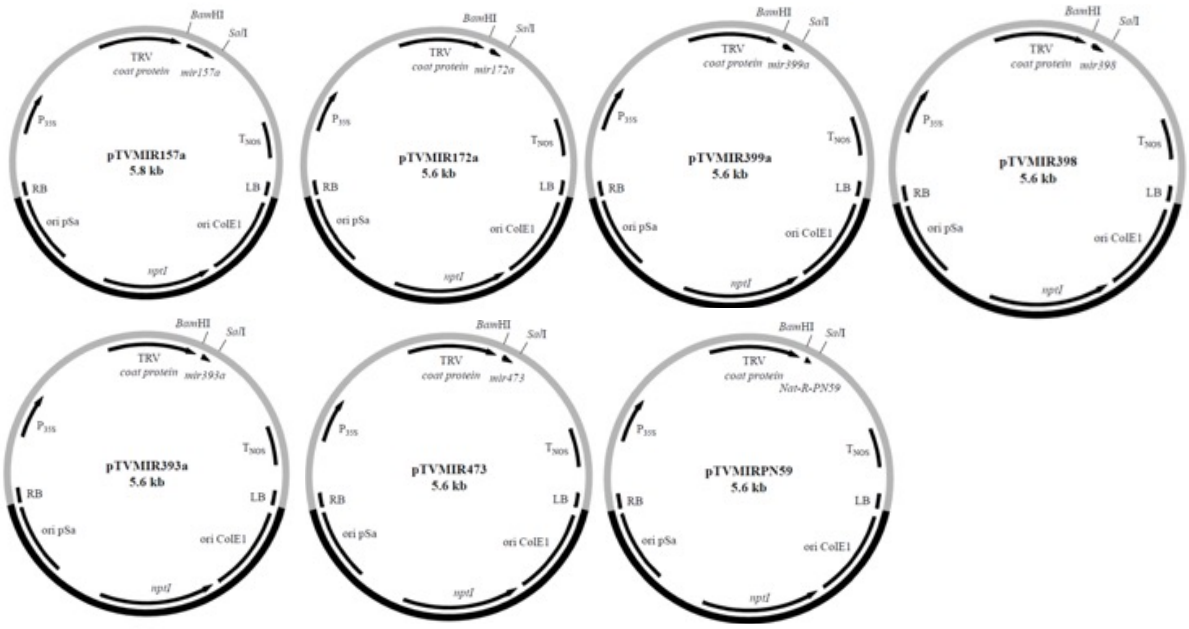

Fig. S10. Transformation vector maps for overexpression of 7 miRNAs for determining their function in plant-AMF interaction.

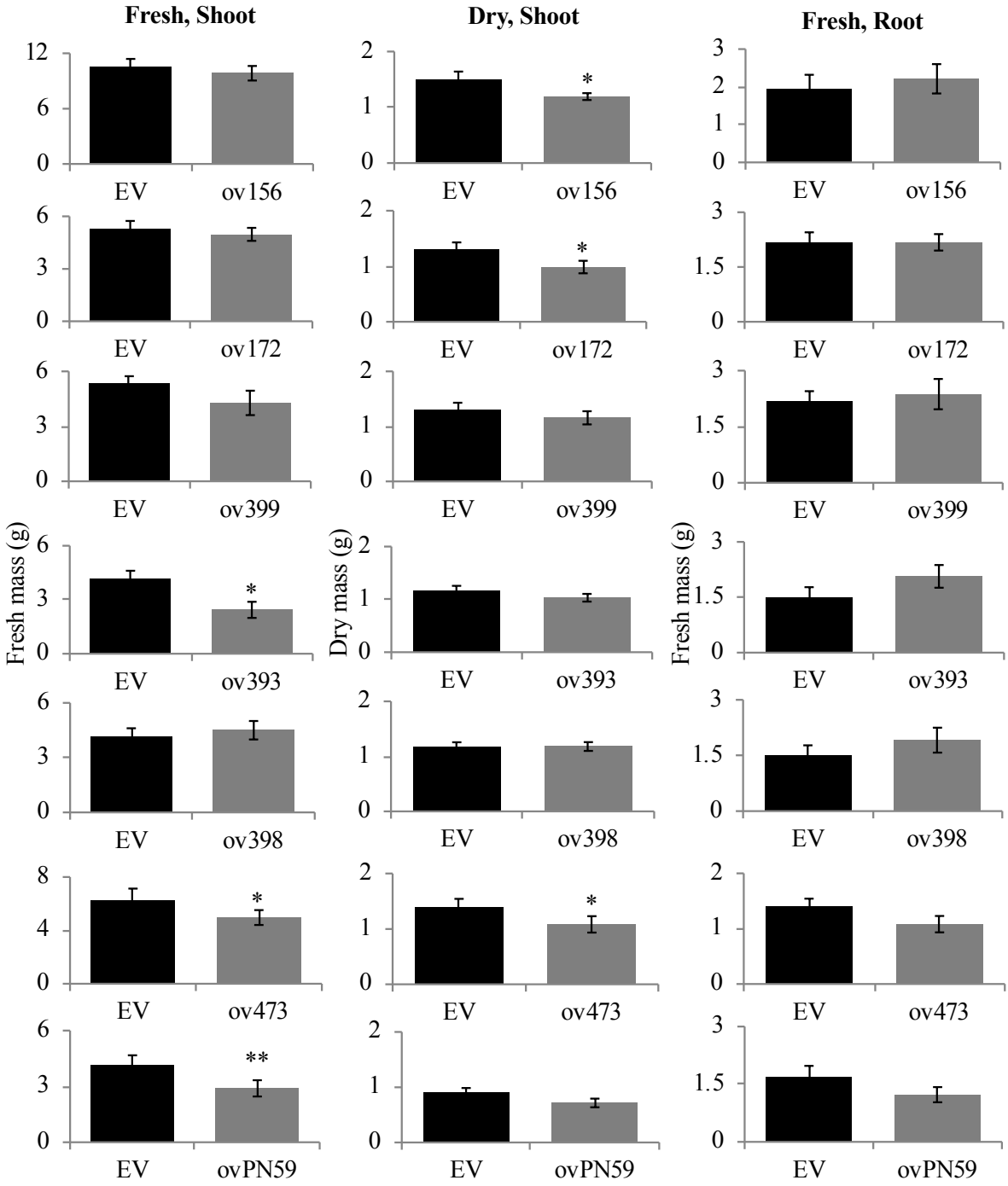

Fig. S11. Evaluation of shoot and root biomass of *N. attenuata* plants over-expressing 7 miRNAs compared to the EV counterparts. Significant differences were evaluated with the help of one-way ANOVA. Values presented are means ± SD, number of biological replicates (n) =8-12; * and ** show significant differences at P<0.05 and P<0.01, respectively; ov156-EV comparison for dry shoot mass: F=6.57, P=0.03; ov172-EV for dry shoot mass: F=5.32, P=0.031; ov393-EV for fresh shoot mass: F=6.45, P=0.031; ov473-EV for fresh shoot mass: F=7.21, P=0.032; ov473-EV for dry shoot mass: F=6.35, P=0.030; ov-Nat-R-PN59 for fresh shoot mass: F=7.67, P=0.01.

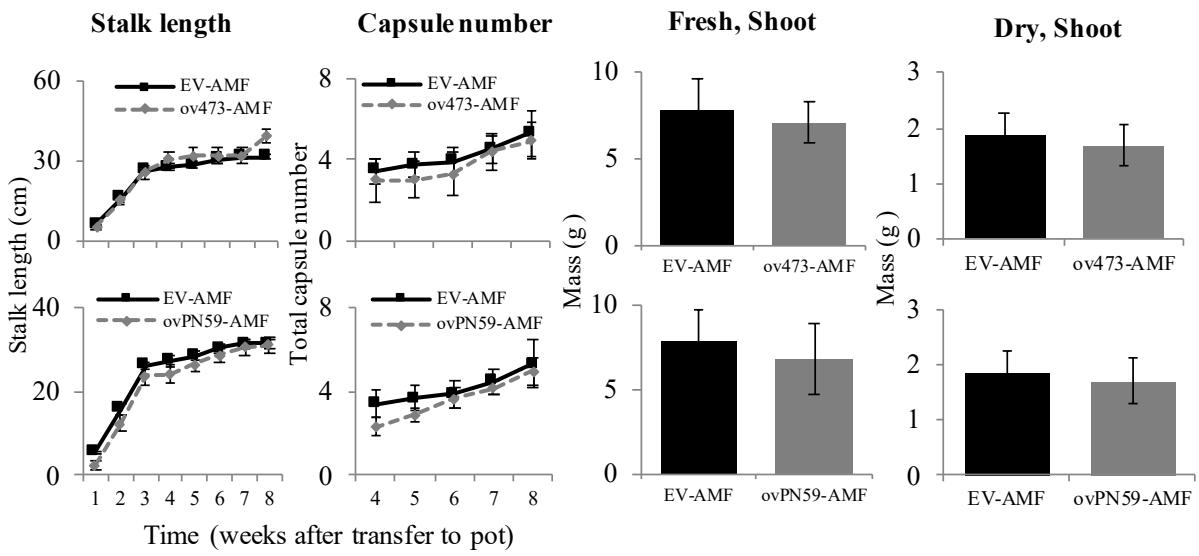

Fig. S12. Phenotypic characterization of plants over-expressing miR473 and PN-59 in absence of AMF. No statistically significant differences were recorded. Two-way repeated measures ANOVA was used for stalk length and capsule numbers, and one-way ANOVA for fresh and dry shoot mass. Values presented are means ± SD, number of biological replicates (n) =8-12.

Table S1. List of primers ((a) of genes, and (b) of miRNAs) used in this study.

(a) List of primers of genes used in this study

Primer	Forward sequence	Reverse sequence
SPL3	CATCAGCTAAAGAGTACCATCGG	CAGTGTAGCAGGTTCCATGAG
SPL6	TGTAGCAGGTTTCACTTATTGG	GCGAAGAAAGCCTCAATTTG
SPL9	TGCTACACATTCTAAGTCTCCTG	CAGTGTAGCAGGTTCCATCG
SPL12	CACCGAAAGCATCATGTTTGTC	CAGTGTAGCAGGTTCCATAGC
SPL16	ACGTTTGGATGGACATAACAGG	CAGCAAGGGACGAAACTTCT
RAP2-7	AGAAGCTGTTACCAACTTTGAG	CTGAACTTAGGGATTGCGACTT
AP2	TCCTATGAAGAAGAGCCGCC	GTCTCACATATGGGATTGTGGAA
BHLH130	ATGGATAAGCAAACCAACACAG	CCTTCAGAAACAAGTCCAGACA
APL	AGCATCAGAGGAGTCTTCAG	GGGAATTGAGATCACAGAAGC
GLYK	AATGCTGGAAGCCATGATCTC	CCTCGATATGATAAATCTGCGTAC
PEX14	GCTGACAAGTCTGTTAAACTACC	CTGGAAGGGCAAGGTAATACTT
PMT28	CCATCAATGGAGGATTTGCAG	CCCATAGTCTTTGAGCGAGG
GL	CAACAAAGGGAAGATTAGGTGGTC	ACCAAGGCTACGGACAACTT
L4	CTGTAGTTGTTCTAGCTGAATGG	CCTAATGTTTCTGATGCTCACA
IPT 1-4	AAGGATTCGGTATTCTGGGT	CTCCATACAAGGTTGATCCAAT
DELLA	CAAAGTATATGATGGCGAAGTCCT	GGTGCTCTCAACTCTGTTCTG
PAP12	TTCTGGGAGATGAAGCTAAGG	GAGGAAACAAGGGAACTACATTTG
SEC13	CTTGGCTTGTGGTTCTTCAG	GGGACACTACGAGAATTGAC
ALKK	AAGAGTTGCCCTAATTCATGGA	CTGGTGATATTGTGGCAGCA
AFB2	ATTTGTCGTCCCTGAACTTGAG	CGCCTATGGATTCTGGATACC
TIR1	GTTTGCTCCAGACTCACCTC	GGTTGTGGGTGCTAGATTACATT
PUB45	AGAGCCTAAGTTACATGGAGGA	GACCTAGAAGCACATCTGGT
EIN	CATGATCTGAAGAAAGCGTGG	CCGATATTGCTAAGATCCGTAAG
ECI	AGAAACTGCAGGGTACTGTTGG	GAAGGAGGTATAACTGGTGCCC

(b) List of primers of miRNAs used in this study

Primer id	Primer sequence
5SrRNA	CACCGGATCCCATCAGAACT
miR156a-5p_1	TGACAGAAGAGAGCGAGCAC
miR156a-5p_2	TGACAGAAGAGAGTGAGCAC
miR156a-5p_3	TGACAGAAGAGAGTTAGCAC
miR156a-3p	GCTCACTGCTCTATCTGTCACC
miR156b-5p	TTGACAGAAGATAGAGAGCAC
miR156f-3p	TGCTCACTGCTCTATCTGTCACC
miR160-5p	TGCCTGGCTCCCTGTATGCCA
miR165a-3p	TCGGACCAGGCTTCATTCCCC
miR165a-5p	AAATGTTGTTTGTGACGAGTTATT
miR170-3p	TGATTGAGCCGTGCCAATATC

miR171a-3p	TGAGCCGAACCACTATCACTC
miR171b-3p_1	TTGAGCCGCGCCAATATCACG
miR171b-3p_2	TTGAGCCGCGCCAATATCACT
miR172a-3p_1	GGAATCTTGATGATGCTGCAG
miR172a-3p_2	TGAATCTTGATGATGCTGCAT
miR319-5p	AGCTGCCGACTCATTCATTCA
miR390a-3p	CGCTATCCATCCTGAGTTTCA
miR390a-5p	AAGCTCAGGAGGGATAGCGCC
miR393a-3p	ATCATGCTATCCCTTTGGACT
miR393a-5p	TCCAAAGGGATCGCATTGATC
miR398	TGTGTTCTCAGGTCACCCCTT
miR399a-3p_1	CGCCAAAGGAGAGCTGCCCTG
miR399a-3p_2	TGCCAAAGAAGATTTGCCCCG
miR399a-3p_3	TGCCAAAGGAGAGTTGCCCTG
miR403a-3p_1	TTAGATTCACGCACAAACAT
miR403a-3p_2	TTAGATTCACGCACAAACTCG
miR473_5p_1	ACTCTCCCTCAAGGGCTTCTG
miR473_5p_2	ACTCTCCCTCAAGGGCTTCTGGC
miR482d	TTTCCTATGCCACCCATTCCTA
miR5386	TGTCGCTGGATAGATGGCACTT
miR8667	TTTCCAATTCCACCCATTCCTA
Nat-R-PN5	AAACTCCGTGCCCAGTCAAACAGG
Nat-R-PN47	TATTTGATTGGCGTGGCAGAT
Nat-R-PN59	TGTGGGGCGTAGGATCGAGTCA
Nat-R-PN72	TTGTACGAAAGATAAAGATGC
Nat-R-PN77	TTTCCTGTTGGTGATGAGACTA
Nat-R-PN81	TTTGATACGAACCTGAATCGGC

Table S2. Details of miRNA-over expression construct.

Construct/ miRNA name	Primer1 (name and sequence, 5'-3')	Primer2 (name and sequence, 5'-3')	PCR fragments
pTVMIR157a/ mir157a	SRNA34-47 5'-GCGGCGGGATCCTTTTTTATTTTTTTCGGTCCTGAGAAATTAAATGG-3'	SRNA35-37 5'-GCGGCGGTCGACGAAGAGAGGGATAGTTGACTGAAGG-3'	GCGGCGGGATCCTTTTTTATTTTTTTCGGTCCTGAGAAATTAAATGGGCACTGGAAAATGTAAATTTAGGGTAAGGAGTATAGAGGAAGTGGGCAAGAAAGGGTGATAATTGTTGACAGAAGATAGAGAGCACTAATGATGATATGCTAAGTAAATTTAGGGGCAAAAGCATCTCAATTCATTTGTGCTCTCTATGCTTCTGTCATCACCTTCAGTCAACTATCCCTCTCTTCGTCGACCGCCGC
pTVMIR172a/ mir172a	SRNA38-36 5'-GCGGCGGGATCCGAGCATCATCAAGATTCACATAGC-3'	SRNA39-39 5'-GCGGCGGTCGACCTGCAGCATCATCAAGATTCCCATATC-3'	GCGGCGGGATCCGAGCATCATCAAGATTCACATAGCCTTTTTAGGGCTTTTTTGCCCTATGGCTTATTGATATGGGAATCTTGATGATGCTGCAGGTCGACCGCCGC
pTVMIR393a /mir393a	SRNA42-36 5'-GCGGCGGGATCCTCCAAAGGGATCGCATTGATCCTG-3'	SRNA43-34 5'-GCGGCGGTCGACAATCCGAAGAGATCGCATGATC-3'	GCGGCGGGATCCTCCAAAGGGATCGCATTGATCCTGTGTCCCAATTAGAGTCCAATGGGATCATGCGATCTCTTCGGATTGTCGACCGCCGC
pTVMIR398/mir398	SRNA44-35 5'-GCGGCGGGATCCAGTGAACATGGGAACACAGGTGC-3'	SRNA45-35 5'-GCGGCGGTCGACAAGGGGTGACCTGAGAACACAAG-3'	GCGGCGGGATCCAGTGAACATGGGAACACAGGTGCATTTGGGTATTTTTGTTTTGGCTAAAATCTAAATGCACTTGTGTTCTCAGGTCACCCCTTGTCGACCGCCGC
pTVMIR399a/ mir399a	SRNA50-33 5'-GCGGCGGGATCCGGGTTTCTCTTTATTGGCATG-3'	SRNA51-32 5'-GCGGCGGTCGACCAGGGCAACTCTCCTTTGGC-3'	GCGGCGGGATCCGGGTTTCTCTTTATTGGCATGCATTAACTTGGTGACTCTGTTTGATCACAAATATTAGCTGACATGCCAAAGGAGAGTTGCCCTGGTCGACCGCCGC
pTVMIR473/mir473	SRNA48-35 5'-GCGGCGGGATCCACTCTCCCTCAAGGGCTTCTGGC-3'	SRNA49-36 5'-GCGGCGGTCGACCCACTCTCACTCGAAAGACCTCTG-3'	GCGGCGGGATCCACTCTCCCTCAAGGGCTTCTGGCTTAAAATGCTTAATCTTTGGTTTGTGTTAATGCCAGAGGTCTTTCGAGTGAGAGTGGGTCGACCGCCGC
pTVMIRPN59/ mirPN59	SRNA40-33 5'-GCGGCGGGATCCTGTGGGGCGTAGGATCGAGTC-3'	SRNA41-34 5'-GCGGCGGTCGACGATGTAAGGAGTAGATCGAATG-3'	GCGGCGGGATCCTGTGGGGCGTAGGATCGAGTCACATTCGATCTACTCCTTACATCGTCGACCGCCGC

Table S3. Statistical details of parameters tested in Fig. **6**.

Comparison	Trait	Test used	DF	F-Value	P-Value
miR156b-5p-EV	Over-expression	One way ANOVA	19	4.85222	0.04088
	Stalk length	Two way repeated measures ANOVA	45	238.2439	8.80E-08
	Capsule number	Two way repeated measures ANOVA	18	27.773	5.14E-04
	Blumenol C	One way ANOVA	19	6.67508	0.01365
miR172-3p_1-EV	Over-expression	One way ANOVA	19	73.78256	8.77E-08
	Stalk length	Two way repeated measures ANOVA	63	233.9019	9.53E-08
	Capsule number	Two way repeated measures ANOVA	36	62.90177	2.37E-05
	Blumenol C	One way ANOVA	19	2.07952	0.16646
miR399a-3p_3-EV	Over-expression	One way ANOVA	18	37.59708	1.11E-05
	Stalk length	Two way repeated measures ANOVA	56	182.6053	8.63E-07
	Capsule number	Two way repeated measures ANOVA	36	57.44657	3.40E-05
	Blumenol C	One way ANOVA	18	6.52019	0.02056
miR393a-5p-EV	Over-expression	One way ANOVA	20	20.62659	2.23E-04
	Stalk length	Two way repeated measures ANOVA	54	154.9338	5.63E-07
	Capsule number	Two way repeated measures ANOVA	27	41.40241	1.20E-04
	Blumenol C	One way ANOVA	20	2.78598	0.05149
miR398-3p-EV	Over-expression	One way ANOVA	20	7.27142	0.0143
	Stalk length	Two way repeated measures ANOVA	54	174.8852	3.35E-07
	Capsule number	Two way repeated measures ANOVA	27	51.56824	5.19E-05
	Blumenol C	One way ANOVA	20	6.47517	0.01978
miR473-5p_2-EV	Over-expression	One way ANOVA	17	40.87557	8.90E-06
	Stalk length	Two way repeated measures ANOVA	45	171.2186	3.67E-07
	Capsule number	Two way repeated measures ANOVA	27	59.08345	3.04E-05
	Blumenol C	One way ANOVA	17	6.47561	0.01003
miRNat-R-PN59-EV	Over-expression	One way ANOVA	17	6.1636	0.02451
	Stalk length	Two way repeated measures ANOVA	45	143.9884	7.70E-07
	Capsule number	Two way repeated measures ANOVA	27	54.14917	4.29E-05
	Blumenol C	One way ANOVA	17	7.67508	0.01365

Methods S1. Detailed description of the materials and the methods used in this study.

Plant material and glasshouse growth conditions

Seeds of the 31st generation of an inbred *N. attenuata* Torr. Ex Watts wild-type plant (WT), originally collected from southwestern Utah, USA were used for all experiments. Two independent transgenic ir*AGO7* lines (A-13-018-8-4 and A-13-017-2-2) have been described previously and did not show any significant differences among each other (Pradhan *et al.*, 2017). Therefore, we randomly selected line A-13-018-8-4 for the experiments presented here. Generation and characterization of all the irAGO genotypes have been described in previous studies (Pradhan *et al.*, 2017; Pradhan *et al.*, 2020). *N. attenuata* plants transformed with empty vector construct (EV) do not show any significant differences from the WT in ecologically relevant traits (Pandey and Baldwin, 2007; Schwachtje et al. 2008). Hence, WT served as an appropriate control genotype against which to compare the performance of irAGO lines (Pandey and Baldwin, 2007; Schwachtje *et al.*, 2008; Pradhan *et al.*, 2017; Pradhan *et al.*, 2020). Seeds from WT and all the transgenic plants (ir*AGO1* [A-12-866-1-5], ir*AGO2* [A-12-845-2-8], ir*AGO4* [A-13-021-2-6], ir*AGO7* [A-13-018-8-4], ir*AGO10* [A-13-025-6-7]) were germinated on Gamborg B5 medium as previously described (Krügel *et al.*, 2002). Plants were grown and maintained under a day/night cycle of 16 h (26 to 28°C)/8 h (22 to 24°C) and 45 to 55% humidity (Krügel *et al.*, 2002; Halitschke *et al.*, 2003; Onkokesung *et al.*, 2012).

For the glasshouse experiments with AMF, plants were first transferred to sand in Teku pots, and 10-12 days later into inactive (autoclaved twice at 121 °C for 30 min; non-inoculated controls) or living inoculum (*R. irregularis*, Biomyc Vital, www.biomyc.de, inoculated plants), diluted 1:10 with expanded clay (size: 2-4 mm). Plants were watered with distilled water for the first day of pot transfer and then fertilized every second day with a low phosphate (P) hydroponic solution (Groten *et al.*, 2015) containing 1/10 of the regular inorganic P concentration during rosette stage growth, and starting with the elongation stage with 1/4 P concentration (Wang *et al.*, 2017). One L of regular hydroponic solution (full strength) contained 0.1292 g $CaSO_4 2H_2O$, 0.1232 g $MgSO_4$, 0.0479 g K_2HPO_4, 0.0306 g KH_2PO_4, 2 mL KNO_3 (1M), 0.5 mL micronutrient, 0.5 mL Fe diethylene triamine penta-acetic acid (Groten *et al.*, 2015).

For experiments presented in Fig. **2a**, all plants were grown in standard soil conditions, in 1 L pots without competition (Krügel *et al.*, 2002). Plant performance in terms of rosette diameter, chlorophyll content, stalk length, total capsule number, and shoot and root fresh mass, were recorded at several time points. For experiments presented in Fig. **2b** and onward, plants were subjected to resource-limited conditions by growing them in initially size-matched pairs in 2 L pots, in expanded clay with AMF inoculum and low-P as described above. A WT plant was always paired with an irAGO7 size-matched plant in the same pot to allow the two genotypes to compete for resources as previously described (Pandey *et al.*, 2008b). During sample harvests, roots were carefully washed, briefly dried with a paper towel, cut into approximately 1 cm long pieces and mixed. An aliquot was stored in root storage solution (99% ethanol and 60% acetic acid, 3:1, v:v) at 4°C for microscopic analysis, while the remaining root material was immediately frozen in liquid nitrogen and stored at -80°C for future use.

Blumenol analysis and microscopic observations for estimating host-AMF interaction

11-Carboxyblumenol-C-glucoside is a reliable quantitative marker for root colonization of AMF (Wang *et al.*, 2018b). For the quantification of 11-carboxyblumenol-C-glucoside contents, weighed leaf samples were aliquoted into reaction tubes, containing two steel balls. For 100 mg plant tissues, approximately 1 mL 80% MeOH was added to the samples, and shaken in a GenoGrinder 2000 (SPEX SamplePrep) for 60 s at 1150 strokes min^{-1}. After centrifugation, the supernatant was collected and analyzed with a ultra-high performance liquid chromatography (UHPLC), using a Dionex UltiMate 3000 rapid separation LC system (Thermo Fisher) as described in detail previously (Wang *et al.*, 2018b).

To determine the fungal colonization rates and mycorrhizal structures, root samples were stained and analyzed by microscopy. Roots were first washed with distilled water and then boiled in a 2% (w/v) KOH solution for 5 min. After rinsing with water, the roots were boiled in 2% HCl solution for 5 min, rinsed with water and subsequently stained with Trypan blue as previously described (Brundrett *et al.*, 1984; McGonigle *et al.*, 1990) to visualize mycorrhizal structures. For the quantification of mycorrhizal colonization, 10 root fragments, each about 1 cm long, were stained with either Trypan blue and mounted on a slide. Approximately 150

view fields per slide were surveyed with an Axioskop/Zeiss Imager.Z1 in 200x magnification; visible structures were classified into three groups: arbuscules, vesicles and hyphae as described in McGonigle *et al.* (1990). Additionally, mycorrhizal roots and fungal structures were stained by using WGA-fluorescein (WGA-FITC; Rech et al., 2013). The staining was conducted on samples collected at a time-point of 6-weeks after inoculation. The roots were treated with 10% KOH for 45 min at 90 ^{0}C and neutralized with 1% HCl at room temperature. After three washes with 1X PBS, roots were submerged in staining solution (5µg ml^{-1} WGA-Fluorescein in 1 X PBS) overnight at 4°C. These were washed (1X PBS) and analyzed under a Leica TCS SP5 (DM5000) confocal microscope (http://www.leica-microsystems.com/). The data was analyzed as described in Trouvelot et al. (1986).

RNA extraction and quantitative real time PCR and miRNA target identification

To analyze miRNA accumulation and gene expression, approximately 200 mg of powdered root sample was used for RNA extraction. Total RNA was extracted from the root samples using the lithium chloride method as previously described by Kistner & Matamoros (2005) and adapted to *N. attenuata* (Pradhan *et al.*, 2017).

To quantify miRNA transcript abundance, a total of 1 µg of total RNA was converted to cDNA according to the manufacturer's instruction (www.qiagen.com). Real-time qPCR was performed on a Mx3005P qPCR system (Stratagene, Santa Clara, CA, USA; http://www.stratagene.com). qPCR was performed with the help of miScript SYBR Green PCR kit, following the manufacturer's protocol. qPCR assays were performed using the specific miRNA sequences from Pandey *et al.* (2018). A total of 10 ng of cDNA was used to detect miRNA in each sample. 5S rRNA gene was used for normalization of microRNA transcript abundances by real-time reverse transcription (RT) PCR. The $2^{-\Delta\Delta CT}$ method was used for data analysis (Bubner & Baldwin, 2004). Details of miRNA locations, origin, orientation, conservation and putative targets have been presented in Pandey *et al.* (2018).

For mRNA quantification, RT was performed using oligo (dT) and Superscript II reverse transcriptase according to the manufacturer's instruction (www.invitrogen.com). Real-time qPCR with the help of qPCR core kit for Taykon™ SYBR master mix, (Eurogentec), following the manufacturer's protocol. qPCR assays were performed using gene-specific primers (designed with the help of Primer Express software v 3.0.1; http://www.appliedbiosystems.com) on cDNA

templates corresponding to 50 ng total RNA before reverse-transcription. The *N. attenuata* sulfite reductase (*ECI*), a housekeeping gene, was used as an endogenous reference (Bubner & Baldwin, 2004; Bubner *et al.*, 2004). The $2^{-\Delta\Delta CT}$ method was used for data analysis (Bubner *et al.*, 2004). For determining relative transcript abundances, levels corresponding to time point 0 hpi (hours post inoculation; controls) were set to 1 (as reference) to standardize relative transcript abundances at various time points (Bubner & Baldwin, 2004; Pandey & Baldwin, 2007; Bozorov *et al.*, 2012). *N. attenuata* plants, when grown under P-limited conditions without AMF, are severely stressed, their vegetative growth phase is extremely shortened, and they produce only a few capsules. These developmentally-accelerated and stressed plants do not serve as suitable controls and we used the values at 0 hpi to normalize abundances. Here, all plants of both the genotypes were developmentally matched.

Targets of miRNAs were chosen from a previous study that identified them during plant-AMF interaction in *N. attenuata* (Pandey *et al.*, 2018). miRNA-mRNA interactions were investigated and a network was constructed according to the protocol previously published (Pandey *et al.*, 2019), and applied to study AGO-mediated miRNA's role in other host-environmental interactions (Pradhan *et al.*, 2017; Pradhan *et al.*, 2020).

A list of sequences of all the primers (genes and miRNAs) used in the study is provided in Table S1.

Field experiments

All field experiments were conducted at the Lytle Ranch Preserve, located in the Great Basin Desert of Southwestern Utah, USA (latitude 37.146, longitude 114.020) in two consecutive years: 2018 and 2019. The release of transgenic plants was conducted under APHIS importation and release permits (18-054-101r and 18-282-103r). Seeds were germinated directly on borax-soaked Jiffy 703 pots (AlwaysGrows), which were planted into the field plot 3 to 4 weeks later. 10-15 pairs of size-matched seedlings of WT and ir*AGO7* (A-13-018-8-4) genotypes were planted. Plants in a pair were planted 20-30 cm apart in a quadrant design surrounding a centrally located irrigation dripper; quadrants were randomized over the field plot to avoid any spatial variation in the diversity of root-associated microbial communities that remained after the field plots had been deep plowed and harrowed

in six directions to randomize the soil conditions across the plot. Rosette diameters were measured one week onwards; as 3 weeks after transplanting, the plants started to elongate, measurements of the stalk length, flower number and the initiation of capsule set was quantified at regular weekly intervals until 7-8 weeks after transplantation. Herbivory was estimated as the percentage of total plant canopy area of WT and ir*AGO7* plants damaged at 4 and 8 weeks. Susceptibility of plants to natural pathogens was quantified by monitoring mortality as previously described (Pradhan *et al.*, 2020). Experiments were terminated after 8 weeks (when the plants started to produce seed capsules) by uprooting the plants. All seed capsules were removed before they matured to meet the regulatory requirements. Total flower counts were used for fitness estimates, and total biomass values were estimated by carefully excavating roots from the soil, separating shoots from roots, which were washed with water. After air drying, the cleaned roots and shoots were weighed.

Statistical analysis

Data were analyzed using OriginLab 2016 software. All the fitness-related parameters (rosette diameters, stalk lengths, fresh and dry biomass, and total flower number (field), and seed capsules produced from the competition experiments were analyzed using paired T-tests; gene expression and miRNA expression data were analyzed by ANOVA (one-way and repeated measures wherever applicable).

Transient over-expression of Na-miRNAs

N. attenuata miRNAs were transiently over-expressed. We needed a system where specific miRNAs were over-expressed throughout the duration of colonization (up to 8 weeks). Further, we needed a setup that could systemically transit the miRNA signal to the plant's roots and could be high-throughput so that we could examine the biological function of several miRNAs. Most importantly, we did not want the over-expression of miRNAs to interfere with seed germination, development and differentiation of roots. We found that using an approach that was similar to VIGS technology (using a viral vector, pTV00, based on the Tobacco Rattle Virus; Ratcliff *et al.*, 2001; Saedler & Baldwin, 2004) was able to address the above-mentioned requirements. We found that the over-expression of miRNAs continued through 6-8 weeks of the study period. To minimize the possibility of generating a series of small RNAs from the miRNA-backbone, we had exposed the miRNA

backbone sequence (the sequence present in the pTVMIR construct) to both the SGN VIGS tool (Fernandez-Pozo et al., 2015) and a BLAST search against the complete transcriptome of *N. attenuata*. The analysis did not return any small RNAs (>18 nt) from the input sequences and we inferred that the approach led to the '*in planta* expression of specific miRNAs'.

Vector construction involved the following steps. Genomic DNA (gDNA) was isolated from leaves of one rosette stage *N. attenuata* plant (genotype Utah 30x, SAMN04590212) by a modified cetyltrimethylammonium bromide method (Bubner *et al.*, 2004). The pre-microRNA genes were PCR amplified from gDNA of *N. attenuata* using Phusion DNA Polymerase (www.thermofisher.com) according to the instructions of the manufacturer. The obtained PCR fragments (68 bp to 245 bp) were cloned as *Bam*HI – *Sal*I fragments in vector pTV00 (Ratcliff *et al.*, 2001) cut with the same enzymes. The sequences of the PCR primers and PCR fragments used for the indicated constructs and microRNAs are provided in Table S2.

Using electroporation, *Agrobacterium tumefaciens* GV3101 was transformed with the constructs and syringe-infiltrated into leaves. Empty vector- (EV) constructs were used as controls, and 10 biological replicates (plants) were independently inoculated with each construct. Plants were grown in sand pots; fourteen days after transformation, plants were transferred to 10% AMF inoculum as described earlier (Groten *et al.*, 2015). Plants over-expressing individual miRNAs and the corresponding EV controls were grown each in 1L pots in a growth chamber under P-limited conditions with AMF as described above for 6-8 weeks; growth, and fitness parameters were recorded weekly until harvest; AMF colonization was monitored at 6 and 8-weeks by analyzing blumenol-C contents as described above. Over-expression was quantified in individual plants with the miRNA qPCR assays as described above.

Bozorov TA, Baldwin IT, Kim S-G. 2012. Identification and profiling of miRNAs during herbivory reveals jasmonate-dependent and -independent patterns of accumulation in Nicotiana attenuata. *BMC plant biology* **12**: 209-209.

Brundrett MC, Piché Y, Peterson RL. 1984. A new method for observing the morphology of vesicular–arbuscular mycorrhizae. *Canadian Journal of Botany* **62**(10): 2128-2134.

Bubner B, Baldwin IT. 2004. Use of real-time PCR for determining copy number and zygosity in transgenic plants. *Plant Cell Reports* **23**(5): 263-271.

Bubner B, Gase K, Baldwin IT. 2004. Two-fold differences are the detection limit for determining transgene copy numbers in plants by real-time PCR. *BMC Biotechnol* **4**(1): 1-14.

Fernandez-Pozo N, Rosli HG, Martin GB, Mueller LA. 2015. The SGN VIGS tool: user-friendly software to design virus-induced gene silencing (VIGS) constructs for functional genomics. *Molecular Plant* **8**: 486-488

Groten K, Nawaz A, Nguyen NHT, Santhanam R, Baldwin IT. 2015. Silencing a key gene of the common symbiosis pathway in Nicotiana attenuata specifically impairs arbuscular mycorrhizal infection without influencing the root-associated microbiome or plant growth. *Plant Cell Environ* **38**(11): 2398-2416.

Halitschke R, Gase K, Hui DQ, Schmidt DD, Baldwin IT. 2003. Molecular interactions between the specialist herbivore *Manduca sexta* (Lepidoptera, Sphingidae) and its natural host *Nicotiana attenuata.* VI. Microarray analysis reveals that most herbivore-specific transcriptional changes are mediated by fatty acid-amino acid conjugates. *Plant Physiol* **131**(4): 1894-1902.

Kistner C, Matamoros M 2005. RNA isolation using phase extraction and LiCl precipitation. In: Márquez AJ, Stougaard, J., Udvardi, M., Parniske, M., Spaink, H., Saalbach, G., Webb, J., Chiurazzi, M., Márquez, A.J. ed. *Lotus Japonicus Handbook*. Netherlands: Springer, 123-124.

Krügel T, Lim M, Gase K, Halitschke R, Baldwin IT. 2002. *Agrobacterium*-mediated transformation of *Nicotiana attenuata*, a model ecological expression system. *Chemoecology* **12**(4): 177-183.

McGonigle TP, Evans DG, Miller MH. 1990. Effect of degree of soil disturbance on mycorrhizal colonization and phosphorus absorption by maize in growth chamber and field experiments. *New Phytologist* **116**(4): 629-636.

Onkokesung N, Gaquerel E, Kotkar H, Kaur H, Baldwin IT, Galis I. 2012. MYB8 controls inducible phenolamide levels by activating three novel hydroxycinnamoyl-coenzyme A:polyamine transferases in *Nicotiana attenuata*. *Plant Physiol* **158**(1): 389-407.

Pandey P, Wang M, Baldwin IT, Pandey SP, Groten K. 2018. Complex regulation of microRNAs in roots of competitively-grown isogenic Nicotiana attenuata plants with different capacities to interact with arbuscular mycorrhizal fungi. *BMC Genomics* **19**(1): 937.

Pandey P, Srivastava PK, Pandey SP. 2019. Prediction of plant miRNA targets. *Methods Mol Biol.* 1932:99-107.

Pandey SP, Baldwin IT. 2007. RNA-directed RNA polymerase 1 (RdR1) mediates the resistance of Nicotiana attenuata to herbivore attack in nature. *Plant J* **50**(1): 40-53.

Pandey SP, Gaquerel E, Gase K, Baldwin IT. 2008b. RNA-directed RNA polymerase3 from *Nicotiana attenuata* is required for competitive growth in natural environments. *Plant Physiol* **147**(3): 1212-1224.

Pradhan M, Pandey P, Baldwin IT, Pandey SP. 2020. Argonaute 4 modulates resistance to Fusarium brachygibbosum infection by regulating jasmonic acid signaling. *Plant Physiol*: pp.00171.02020.

Pradhan M, Pandey P, Gase K, Sharaff M, Singh RK, Sethi A, Baldwin IT, Pandey SP. 2017. Argonaute 8 (AGO8) Mediates the Elicitation of Direct Defenses against Herbivory. *Plant Physiol* **175**(2): 927-946.

Ratcliff F, Martin-Hernandez AM, Baulcombe DC. 2001. Technical Advance: Tobacco rattle virus as a vector for analysis of gene function by silencing. *The Plant Journal* **25**(2): 237-245.

Rech SS, Heidt S, Requena N. 2013. A tandem Kunitz protease inhibitor (KPI106)–serine carboxypeptidase (SCP1) controls mycorrhiza establishment and arbuscule development in Medicago truncatula. *The Plant Journal* **75**(5): 711-725.

Saedler R, Baldwin IT. 2004. Virus-induced gene silencing of jasmonate-induced direct defences, nicotine and trypsin proteinase-inhibitors in *Nicotiana attenuata*. J Exp Bot **55**(395):151-7.

Schwachtje J, Kutschbach S, Baldwin IT. 2008. Reverse genetics in ecological research. *PLOS ONE* **3**(2): e1543.

Trouvelot A, Kough J, Gianinazzi-Pearson V 1986. Mesure du taux de mycorhization VA d'un système radiculaire. Recherche de méthode d'estimation ayant une signification fonctionnelle. *Physiological and genetical aspects of mycorrhizae: proceedings of the 1st european symposium on mycorrhizae, Dijon, 1-5 July 1985*. 217-221.

Wang M, Schäfer M, Li D, Halitschke R, Dong C, McGale E, Paetz C, Song Y, Li S, Dong J, et al. 2018b. Blumenols as shoot markers of root symbiosis with arbuscular mycorrhizal fungi. *eLife* **7**: e37093.

Wang M, Wilde J, Baldwin IT, Groten K. 2017. *Nicotiana attenuata*'s capacity to interact with arbuscular mycorrhiza alters its competitive ability and elicits major changes in the leaf transcriptome. *J Integr Plant Biol* **60**(3): 242-261.